Ain Shams Engineering Journal 12 (2021) 2135–2144

Contents lists available at ScienceDirect

Ain Shams Engineering Journal

journal homepage: www.sciencedirect.com

Engineering Physics and Mathematics

Electric and magnetic properties of cobalt, copper and nickel organometallic complexes for molecular wires

Rehab I. Yousef [a], Naglaa F.H. Mahmoud [a], Fouad I. El-Hosiny [a], Fritz E. Kühn [b], Ghada Bassioni [c,*]

[a] Chemistry Department, Faculty of Science, Ain Shams University, Abbassia, 11566 Cairo, Egypt
[b] Department of Chemistry/Catalysis Research Center, Technische Universität München (TUM), Lichtenbergstr. 4, D-85747 Garching bei München, Germany
[c] Chemistry Division, Faculty of Engineering, Ain Shams University, P. O. Box 11517, Cairo, Egypt

ARTICLE INFO

Article history:
Received 20 April 2020
Revised 17 November 2020
Accepted 9 December 2020
Available online 1 January 2021

Keywords:
Nitrile ligands
Schiff base
Organometallic complexes
Molecular wires

ABSTRACT

This research aims at the electric and magnetic characterization of specific organometallic complexes for the purpose of using them as molecular wires confined in specific channels that can find applications in electronic systems. The hybrid inorganic–organic materials are organometallic complexes from different ligands (2-amino-6- (*tert*-butyl)-4-(4-methoxyphenyl)-5,6,7,8-tetrahydroquinoline-3-carbonitrile, Propanedinitrile, 2-[(3-chlorophenyl)methylene and 1H-Isoindole-1,3(2H)-dione, 2-[(1Hindol-3-ylmethy lene)amino]) with different metal ions cobalt, copper and nickel, respectively. These compounds are synthesized and characterized chemically, electrically and magnetically in correlation to systematic changes of functional groups in order to tailor-for-the-purpose the electronic and magnetic behavior of these complexes.
© 2020 The Authors. Published by Elsevier B.V. on behalf of Faculty of Engineering, Ain Shams University. This is an open access article under the CC BY-NC-ND license (http://creativecommons.org/licenses/by-nc-nd/4.0/).

1. Introduction

Molecular wires (or sometimes called molecular nanowires) are molecular chains that conduct electric current. They are the proposed building blocks for molecular electronic and optoelectronic devices to replace metal and silicon-based wires in semiconductor devices. So the promising candidates for molecular wires are those with large delocalized π-systems. Polyene consisting of alternating sequence of single and double bond forming a π-system is the simplest chain to be used as a wire. The aromatic building blocks like polybenzene, combination of aromatic building blocks with conjugated double or triple bonds, represent π-type systems which mimic wire function. In coordination complexes the two different mechanisms responsible for electron transfer are inner and outer sphere electron transfers redox reactions. Organometallic complexes keep one key element that is the unpaired electron spins. These unpaired electrons are introduced by the residing of metal ions which usually carry d-/f- electrons [1,2]. The structural information of the organometallic complexes is an important aspect and the design of the metal–organic complexes is a great challenge because the existence of strong magnetic properties, e.g., ferromagnetism, usually comes along with ordered stacking of molecules which is critical to get unpaired spins aligned up [3]. Both conductivity and magnetism can also be achieved in some exquisite systems. In those cases, organometallic complexes show potential applications in spintronics in which the electrical transport properties can be affected by internal or external magnetic field. Among the wide variety of high-nuclearity coordination compounds with paramagnetic transition metal ions, the cyanide-bridged complexes have attracted the attention of a great number of researchers [4]. The interest is due to the ambidentate character of the cyanide ligand which allows the synthesis of heterometallic compounds and the propagation of exchange magnetic coupling [5,6]. An example for cyano complexes are the 2-Amino-3-cyano-4-(H) pyran derivatives [7,8] which are used as building blocks for important heterocycles synthesis as pyrazopyranopyrimidines [9], chromenooxazine [10], and pyrrolopyranopyrazole [11]. The nitrile ligands included in our work are of great interest nowadays in several fields and synthesized in a way similar to what is recently published [12]. Due to the excellent selectivity, sensitivity and stability for specific metal ions such as Co(II), Cu(II) and Ni(II) a large number of different Schiff base ligands have been used in

* Corresponding author.
E-mail address: ghada_bassioni@eng.asu.edu.eg (G. Bassioni).
Peer review under responsibility of Ain Shams University.

Production and hosting by Elsevier

https://doi.org/10.1016/j.asej.2020.12.002
2090-4479/© 2020 The Authors. Published by Elsevier B.V. on behalf of Faculty of Engineering, Ain Shams University.
This is an open access article under the CC BY-NC-ND license (http://creativecommons.org/licenses/by-nc-nd/4.0/).

potentiometric sensors (as cation carriers), in optical computers, in imaging systems and in the molecular memory storage [13]. In the current study, we report the synthesis of Cu(II), Co(II) and Ni(II) complexes to be suitable for using them in electronic systems, optical systems and data storage devices. The complexes prepared include the nitrile and Schiff base ligands mentioned above (see Scheme 1).

2. Experimental section

All chemicals were purchased and used without further purification and all the electrical, magnetic and some chemical investigations were carried out in the Nanolab units at MESA + Research Institute for Nanotechnology, University of Twente in The Netherlands. Other experiments were carried out in the organic chemistry lab at the Faculty of Science, Ain Shams University and in the Microanalytical lab at the Technical University of Munich in Germany.

2.1. Materials

The reagents and solvents used in the chemical syntheses were of analytical grade. Methanol 99.9%, toluene 99.8+%, dichloromethane 99.8+%, acetonitrile 99.5%, ethanol 100% with 5% methanol, chloroform 99.8+%, ammonium acetate 98+%, ethylene glycol 99+%, and dimethylsulfoxide (DMSO) 99+% were obtained from Acros Organics Company. Cobalt acetate, copper acetate and p-t-butyl cyclohexanone were obtained from Fluka Company while nickel acetate, indole-3-carboxaldhyde, N-aminophthalimide, 1,2 dicyanoethylene, p-anisaldehyde, malononitrile, and 3-chlorobenzaldhyde were obtained from Merck company.

2.2. Methods

2.2.1. Preparation of ligands

Preparation of Nitrile ligand (a). "2-amino-6-(*tert*-butyl)-4-(4-methoxyphenyl)-5,6,7,8-tetrahydroquinoline-3-carbonitrile".

According to [14] an equimolar mixture of p-anisaldehyde (10 mmol, 1.36 mL), malononitrile (10 mmol, 0.66 g), p-t-butyl cyclohexanone (10 mmol, 1.54 g) and excess of Ammonium Acetate in ethylene glycol (30 mL) was heated by microwave for 5 min. The precipitate was filtered off and recrystallized from ethanol to give the solid.

m.p. (160–162 °C). Anal. Calcd. for $C_{21}H_{25}N_3O$ (335): C, 75.22; H, 7.46; N, 12.537. Found: C, 74.80; H, 7.31; N, 12.15. FT-IR (KBr) (cm^{-1}): 3403, 3289 (NH_2), 2209 (CN), 1630 (C=N),1613(C=C).^{1}H NMR (DMSO d_6):δ H (ppm) 7.17 (d, 2H, Ar—H.), 7.10 (d, 2H, Ar-H), 5.14 (s, 2H, NH_2, D_2O exchangeable), 3.78 (s, 3H, OCH_3), 2.21, 1.96 (m, 2H, CH_2) 2.10, 2.06 (t, H, CH_2), 2.00, 1.75 (d, 2H, CH_2), 1.13 (m, 1H, CH), 0.816 (s, 9H, $3CH_3$). ^{13}C NMR (75 MHz, DMSO d_6): δ C (ppm) 162.1, 160.2, 159.9, 152.2, 127.6, 127.6, 125.4, 125.2, 112.2, 112.2, 111.7, 87.8, 55.8, 44.7, 33.4, 32.1, 27.9, 27.6, 27.6, 27.6, 25.7. MS, *m*/*z* (%): 335 ($M^{\cdot+}$), 251 (23.3), 278 (100), 57 (54.4).

Preparation of Nitrile ligand (b). Propanedinitrile- 2-[(3-chlorophenyl) methylene]. This ligand is classified as an α-β unsaturated compound, as shown in Fig. 1a, and synthesized by a well-known general procedure [11] as follows, to 1 mol of 3-chlorobenzaldhyde and 1 mol of 1, 2 dicyanoethylene, 20 mL of absolute ethanol are added to the reaction mixture with continuous stirring for 30 min then the product of the reaction mixture is filtered, washed with ethanol and its melting point was measured (113–116 °C).

Preparation of Schiff base ligand (c). 1H-Isoindole-1,3 (2H)-dione, 2-[(1Hindol-3-ylmethylene)amino] as shown in Fig. 1b.

This Schiff base is synthesized by a well-known general procedure [15] as follows; in a 1-L flask 1 mol of N-aminophthalimide was added to 20 mL of absolute ethanol and heated. 1 mol of Indole-3-carboxaldhyde added with continuous stirring then reaction mixture refluxed for 5–6 h. Finally, reaction product was filtered off and washed with ethanol and its melting point was measured.

2.2.2. Synthesis of complexes

2.2.2.1. Synthesis of complex (1) from ligand (a) + Co. The nitrile ligand (a) was reacted with cobalt acetate tetrahydrate ($Co(CH_3COO)_2{\cdot}4H_2O$), with molar ratio (metal:ligand) 2:1, as follows; 2 mmol of metal salt solution added to 1 mmol of ligand solution with heating using hot plate after refluxing reaction mixture, the resulting precipitate was dried and its melting point measured which was found to be in the range of ~ (250–287 °C). Complex solubility carried out and found that the product is insoluble in toluene and acetonitrile and readily soluble in dichloro methane and DMSO.

2.2.2.2. Synthesis of complex (2) from ligand (b) + Cu. The arylidine ligand (b) was reacted with copper acetate tetrahydrate ($Cu(CH_3COO)_2{\cdot}4H_2O$), with molar ratio (ligand:metal) 2:1, as follows; 6 mmol of solid ligand (1.131 g) was dissolved in methanol giving a yellow solution and 3 mmol of metal salt (0.5985 g) dissolved in methanol giving a bluish-green solution, the metal salt solution was added slowly to the stirred ligand solution to give a dark green solution. The reaction mixture was stirred for 15 min and left to crystallize. The melting point was measured for the resulted precipitate and it was found in the range of (120–134 °C) which differed from that of the ligand (113–116 °C). Complex solubility carried out and found that it's readily soluble in chloroform and DMSO.

2.2.2.3. Synthesis of complex (3) from ligand (c) + Ni. The Schiff base ligand (C) ($C_{17}H_{11}N_3O_2$) with molecular weight (289 g/mol) was reacted with nickel acetate ($Ni(CH_3COO)_2{\cdot}4H_2O$) (248.69 g/mol), with molar ratio (ligand:metal) 2:1 as follows; 0.45 mmol of metal salt was dissolved in methanol on cold and 0.9 mmol of ligand was dissolved in methanol by heating on a hot plate with continuous stirring after that the metal salt solution was added to the well-stirred ligand solution.

Scheme 1. General procedure for the Synthesis of 2-amino-6-(*tert*-butyl)-4-(4-methoxyphenyl)-5, 6, 7, 8-tetrahydroquinoline-3-carbonitrile Ligand (a).

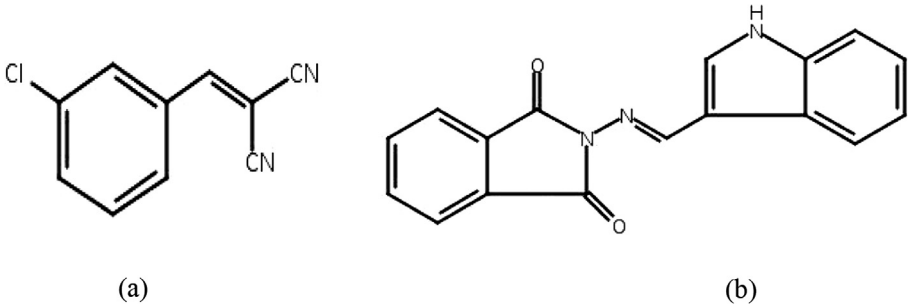

Fig. 1. Structure of ligands (b) and (c).

The resulting mixture refluxed and the color changed after ½ h from yellow to brown then to reddish brown and finally to faint brown after 1 h. After 4 h the amount of precipitate increased and reaction completed after 5 h. The reaction mixture was left to dry for one day in an open air, then filtered and left again to dry. The melting point measured and found to be (325 °C). Complex solubility carried out and found that it's insoluble in toluene & acetonitrile and soluble in dichloromethane when heated and stirred.

2.3. Chemical characterization of the complexes

Elemental analysis for (C, H, N, Co, Cu & Ni) was performed by the Microanalytical Laboratory (Mikroanalytisches Labor) of the Technische Universität München.

Calculations, Geometric optimization of the ligands has been carried out using Chem3D with ChemDraw predefined structures. Geometrical/Energy optimization was carried out using semi-empirical PM3 calculation without any solvent effects in an open shell model and with a maximum RMS value 0.1. Structures of the metal centers were optimized by force field MM2 calculation. Neither charges nor counter ions have been taken into account.

Mass Spectroscopic (MS) investigations were carried using ESI-LCT Mass spectrometer (Waters, Micromass). Complexes were prepared prior to analysis in an Eppendorf vial using 2:1 (mol/mol) ratio and acetonitrile (HPLC gradient grade, VWR) as the solvent. Solutions have been injected using a Hamiltonian syringe with a flow rate of 10 μL/min.

Nuclear Magnetic Resonance (NMR) spectroscopic investigations were carried out at the UT using a 400 MHz instrument equipped with an auto sampler (Bruker). $CDCl_3$ (deuterated chloroform) was used as the solvent and the $CHCl_3$ residues used as internal standard (7.26 ppm).

Calculations, MS and NMR measurements were carried out at MESA + research institute nano lab for nanotechnology, University of Twente, Enschede, Netherlands.

2.4. Physical characterization of the complexes

Drop-casting Method: This was carried out for the complexes samples on glass slit on a hot plate, at 150 °C for samples dissolved in DMSO and under lower temperature 50 °C for samples dissolved in chloroform. Then the samples were kept under N_2 gas and investigated under microscope.

Crystallographic Examination: The drop-casting was carried out on Al_2O_3 slit for each complex after solubility test, then the solvent is evaporated and samples were taken to microscopic examination. For good conductivity measurements results samples should be dissolved completely and form homogenous, continuous and uniform monolayer. After that, samples were taken to undergo spin coating; these investigations were carried out in the nanolab at MESA + research institute for nanotechnology, University of Twente, Enschede, Netherlands.

Spin Coating Method: Al_2O_3 slits were washed with acetone on spinning machine, some of these slits used as it and others coated with hexa methyl disilazane (HMDS) material to form a hydrophobic film on it. Then spin coating was carried out for each complex solution, one on slit without hydrophobic film and second on slit with hydrophobic film then samples are taken to microscopic examination again. Spin coating was carried out in the clean room unit at MESA + research institute for nanotechnology, University of Twente, Enschede, Netherlands.

2.5. Electrical conductivity studies of the Complexes:

Organic Field-Effect-Transistor (OFET) Method: This method was adopted to characterize electrical transport properties of the material. The electrical transport property of complex (1) has been measured at room temperature under reduced pressure (1·10-5-1 ·10-6 mbar) using a JANIS ST-500 Probe station and two Keithley 2400 Source Meters. The platinum electrodes were fabricated on the SiO_2 (100 nm)/Si (p++ substrate. The Si layer was used as a back gate electrode. When sweeping the source-drain voltage (Vsd), a constant bias voltage as the gate voltage (Vgs) to the Si layer (backside of the chip) was applied and the source-drain current (Isd) measured. At the same time, also the gate current (Igs) is monitored to make sure that there was no gate leakage current. The drop-casting was used for deposition of complex (1) onto the IDT-finger electrodes. Before the drop-casting, the acetonitrile was used to disperse the compound (the ratio is 14.7 mg/2 mL).

2.6. Electrical transport measurement method

Electrical transport measurement of the organometallic complexes (1) & (3) junctions was carried out. These junctions were made by drop-casting DMSO solutions of the complexes onto the interdigitated electrodes (Pt). Together with the measurement results, the backside of the devices is p++ silicon which was used as the back-gate. In addition, for some junctions, the light effect on the conductivity was also checked. All measurements were done at room temperature in vacuum (E-5 ~ E-6 mbar) in the proper station.

Complex (1) was dissolved in DMSO and evaporated to form thin film, the temperature increased gradually till 300 K and the current was applied to heat the lamp after evacuation with monitoring the thickness and the rate of deposition, after it remained constant at 0.003 KA° the system was shut down. After waiting till it reached room temperature sample was taken out but it burned completely and no film formed.

2.7. Magnetic conductivity studies of the complexes

Vibrating Sample Magnetometry (VSM). Magnetization curves (M−H curves) of the complexes samples were measured using a vibrating sample magnetometer (VSM, Quantum Design PPMS). In order to obtain reliable data on the magnetic properties of the investigated complexes, a small scaled PET (poly ethylene) tube was used as container for the solid compounds. To prevent movement of powder particle during the vibrating measurement, a small amount of non-magnetic wax was used to remove the background signal from the PET tube and from the wax.

3. Results and discussion

The structure of the synthesized complexes has been identified chemically and physically. Details of the raw data and results obtained are found in the supplementary material.

3.1. Chemical characterization of the complexes

Complex (1): The addition of the cobalt acetate ($Co(CH_3COO)_2 \cdot 4H_2O$) solution to the nitrile ligand (a) with molar ratio 2:1 (metal: ligand) resulted the formation of complex (1).

MS investigation of complex (1): The complex mass spectroscopic pattern shows some of peaks that are of interest, these peaks at (336.2, 392.1 &670.6) mass values. The mass for the ligand (L = 334 g) also (2L = 668 g) & the cobalt acetate salt $Co(AC)_2 \cdot 4H_2O$ with molecular formula ($C_4H_{14}O_8Co$) and molecular mass of (248.93 g) so the molecular mass for (2L + M = 726.93 g), (2L + $Co.CH_3COO$ = 785.93 g) & (L + M = 392.93 g). From the mass spectra for the complex pattern: we found peaks at (336.2, 392.1 & 670.6) that are of nearly equal values for (L = 334, L + Co = 392.93 & 2L = 668) peaks, respectively, so there's fragment for the ligand with the cobalt ion so the complex may be formed by molar ratio 1:1.

Complex (2): The addition of copper acetate (Cu (CH3COO) 2·4H2O) solution to the arylidine ligand (b) with molar ratio 2:1 (Ligand: Metal)/(L: M) resulted the formation of complex (2).

Elemental Analysis study of complex (2) [wt%] (calculated): C: 48.95% (45.40%); H: 3.14% (2.99%); N: 10.36% (7.50%); Cu: 11.1% (17.16%). This indicates that complex (2) has either formula (2L + M.AC) complex or (L + M.(AC)2).

MS investigation of complex (2): The peaks at (128.5, 188.3, 375.9 & 377.9) mass values are important for the structural confirmation, since the mass for the ligand (L = 188.61 g), (2L = 377.22 g), (M/Cu = 63.5 g), the copper acetate molecular mass (Cu.(AC)2 = 1 81.63 g),the acetate (CH3COO/AC) mass is (59 g) & (Cu.(AC) = 12 2.5 g), so the molecular mass for (L + M(AC)2 and (2L + M(AC) are370.24 g and 499.72 g, respectively. From the mass spectra for the complex pattern: we found peaks at (128.5, 188.3, 375.9 & 377.9) that are of nearly equal values for ((M.(AC) = 122.5, L = 188.61, L + M.(AC)2 = 370.24 & 2L = 377.22) peaks respectively and these results agree to some extent with the elemental analysis results.

NMR investigation: From the ^{1}HNMR spectra experimental charts for ligand (b) and for complex (2) we can discuss the following: By comparison of ^{1}HNMR charts for ligand (b) before complexation with its Para-^{1}HNMR chart after complexation with copper we can conclude that there is broadening in the peaks of the ligand in the range (~7.0:12.0 ppm) after complexation, indicating paramagnetism.

Complex (3): The addition of the nickel acetate ($Ni(CH_3COO)_2 \cdot 4H_2O$) solution to the Schiff base ligand (c) with molar ratio 2:1 (ligand:Metal) resulted in the formation of complex (3).

Elemental Analysis for complex (3) [wt%] (calculated): C: 62.09% (62.09%); H: 4.24% (3.60%); N: 11.94% (12.0%); Ni: 8.79% (8.40%). The results account for a chemical formula of (2L + M.(AC)) complex.

MS investigation shows peaks at (113.5 & 278.2) mass values accounting for fragments of (2L + M.(AC) i.e. (2L + Ni.(AC) so these results agree to large extent with the elemental analysis results.

NMR investigation: From ^{1}HNMR spectra experimental charts for ligand (c) and that of complex (3) we can see that the comparison of ^{1}HNMR charts for ligand before complexation with its Para-^{1}HNMR charts after complexation with nickel ion indicates broadening in the peaks in the range (7.0:12.0 ppm) for ligand after complexation.

3.2. Drop casting, crystallographic examination and spin coating studies

The samples were kept under N_2 gas before spin coating and crystallographic pictures were obtained. From the crystallographic results for complexes it can be seen that before spin coating the powder consisted of mainly non-homogenous, non-continuous and non-uniform monolayer, then solution was stirred for 1 h on a hot plate and spin coated. Well adhering monolayer formed which is appropriate for conductivity measurements.

3.3. Electrical conductivity

Electrical Transport Measurement Method: Conductivity measurements carried out directly on the powder sample in the proper station. The sample shows conductivity results (the average result for the current Vs voltage) which was increasing linear relation. Then measurements carried out on the surface of SiO_2 slit with different nano gaps to check its ability to be placed and measured in the logic gate system, results found to be promising for gaps (25 and 35 nm).

After drop-casting and slow baking at (120 °C), the material dried and filled in the gaps between the interdigitated metal fingers. AFM pictures of the IDT electrodes for 39 gaps, ~40 nm gap spacing and 8,1 μm long junction are shown in Fig. 2. Before and after drop-casting are in Fig. 2a & b while 2c is the IV characteristic signal for this junction.

The different results obtained after changing the gap spacing are found in the supplementary material.

3.4. Gate effect measurement:

The gate voltage started from 0 V to +50 V then to −40 V and back to 0 V. The junction was unstably conducting in the beginning when gate biases were set to 0 V, 25 V and 50 V, but turned completely insulating afterwards, no matter what gate bias was applied. So there was little conductivity which is probably due to the electro migration in high source-drain bias region. The junction also shows very tiny conductance. But the conductivity is decreasing monotonically, instead of showing clear gate dependence. The main conclusion is that complex (1) junctions are not completely conducting, even after applying gate biases of +50 V/−40 V.

3.5. Magnetic conductivity

Vibrating Sample Magnetometry (VSM) Method: The complex sample prepared for measurements in a small plastic tube as sample holder, after cleaning in isopropanol and complete drying with compressed air the small tube holder sealed by wax and kept away from any contamination to be ready for measurement. Firstly, the holder and the sample straw were measured alone to check if they are affecting the sample signal or not. Then the sample measured

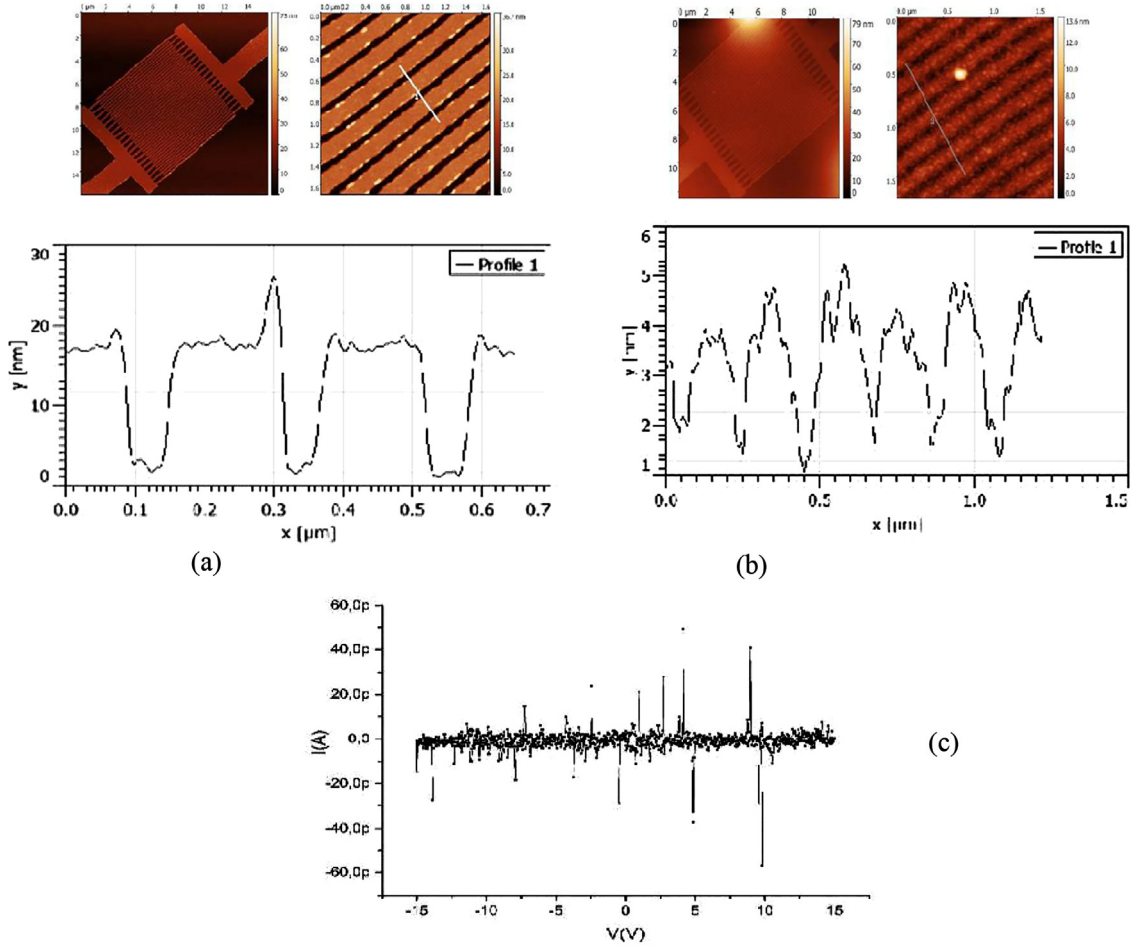

Fig. 2. Complex (1): AFM pictures of IDT electrodes at 39 gaps, ~40 nm gap spacing, ~8.1 μm long (a) before drop casting (b) after drop casting (c) (IV) characteristic signal.

at room temperature (RT) and at 4 K. All the VSM data and plots obtained are shown in the following Fig. 3.

VSM measurement results for Complex (1): The holder was measured alone and showed a small diamagnetic signal. When the sample was measured at room temperature it was found that it gives a paramagnetic signal. From the data above in Fig. 3c, which is zoom in for Fig. 3d, the moment of sample at room temperature increases directly with the applied magnetic field proving its paramagnetism. The signal of the wax and that of the holder are nearly horizontal around zero so cannot greatly affect the sample signal, from Fig. 3b which is a zoom in for Fig. 3a at 4 k we can see the "S" shaped plot but without hysteresis loop so we can't detect exactly if it's ferromagnetic sample or not, but as Co^{2+} itself is paramagnetic assuming that this is due to ion clusters or due to the complex itself. Paramagnetism is a form of magnetism in which material is attracted to an external applied magnetic field and induces internal magnetic field in the same direction of it so those materials have (+ve) magnetic susceptibility (i.e. their magnetic permeability greater than

one/more than that of vacuum (μo) (i.e. ≥1) and their magnetic susceptibility ≥0) and this paramagnetism in the complex refers to presence of unpaired spin electrons .When measurements was carried out at 305 K (RT ~ 32 °C), this means that the thermal motion randomized the spin orientations in the excited state and when temperature decreased to 4 K we can see there is a change in the behavior of the material under magnetic field due to decrease in the thermal effect and decrease of motion. In more details (Paramagnetism is a form of magnetism whereby some materials are weakly attracted by an externally applied magnetic field, and form internal, induced magnetic fields in the direction of the applied magnetic field. In contrast with this behavior, diamagnetic materials are repelled by magnetic fields and form induced magnetic fields in the direction opposite to that of the applied magnetic field. Paramagnetic materials include most chemical elements and some compounds, they have a relative magnetic permeability slightly greater than 1 (i.e., a small positive magnetic susceptibility) and hence are attracted to magnetic fields. The magnetic moment induced by the applied field is linear in the field strength and rather weak. It typically requires a sensitive analytical balance to detect the effect and modern measurements on paramagnetic materials are often conducted with a SQUID magnetometer. Paramagnetism is due to the presence of unpaired electrons in the material, so most atoms with incompletely filled atomic orbitals are paramagnetic, although exceptions such as copper exist. Due to their spin, unpaired electrons have a magnetic dipole moment and act like tiny magnets. An external magnetic field causes the electrons' spins to align parallel to the field, causing a net attraction. Therefore, a simple rule of thumb is used in chemistry to determine whether a particle (atom, ion, or molecule) is paramagnetic or diamagnetic: If all electrons in the particle are paired, then the substance made of this particle is diamagnetic; If it has unpaired electrons, then the substance is paramagnetic. Unlike ferromagnets, paramagnets do not retain any magnetization in the absence of an externally applied magnetic field because thermal motion randomizes the spin orientations. (Some paramagnetic materials retain spin disorder even at absolute zero, meaning they are paramagnetic in the ground state, i.e. in the absence of thermal motion.) Thus the total magnetization drops to zero when the

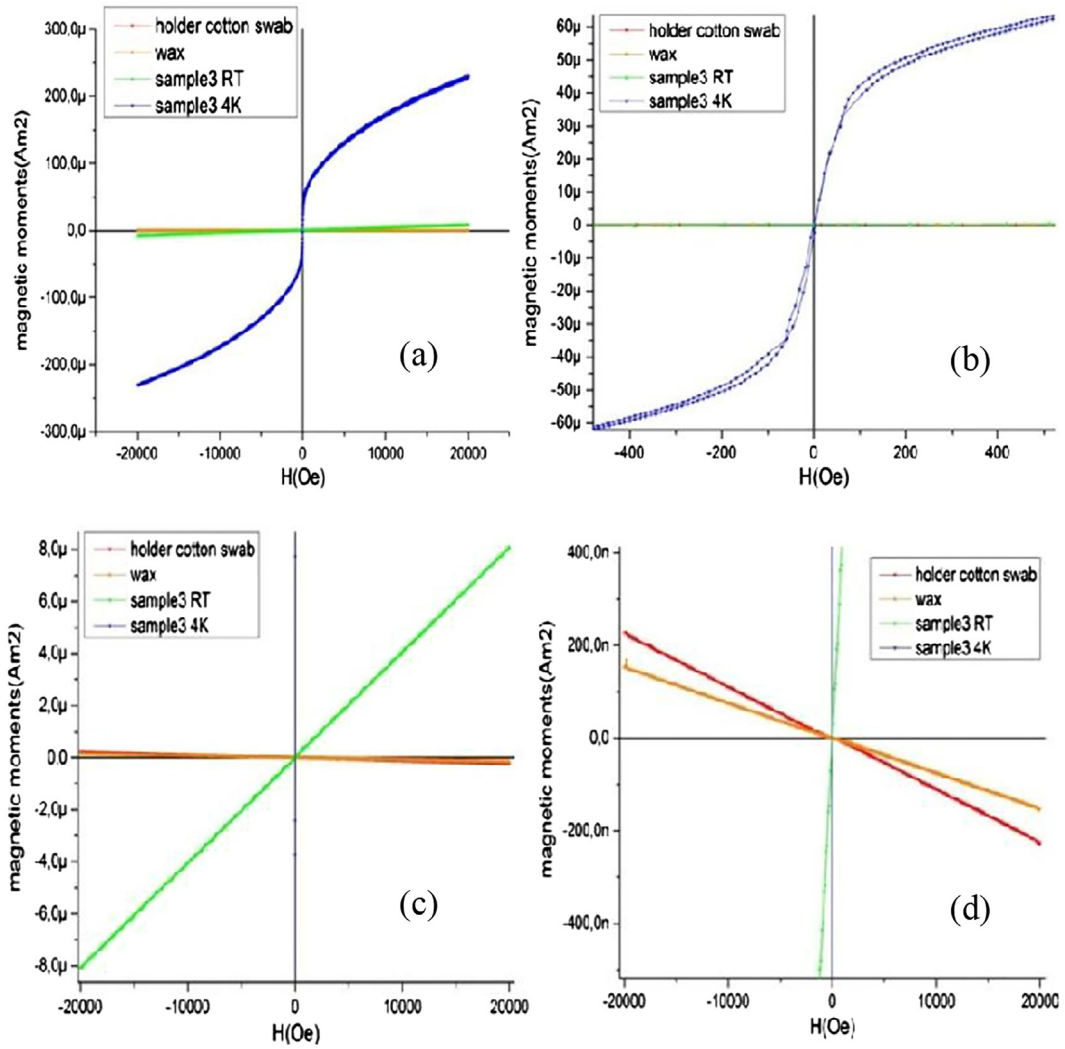

Fig. 3. VSM plots for Complex (1) at RT and 4 K.

applied field is removed. Even in the presence of the field there is only a small induced magnetization because only a small fraction of the spins will be oriented by the field. This fraction is proportional to the field strength and this explains the linear dependency. The attraction experienced by ferromagnetic materials is non-linear and much stronger, so that it is easily observed) [16].

Vibrating Sample Magnetometry (VSM) Method: The complex sample was prepared for VSM measurements as what done for complex (1). All the VSM data and plots obtained are shown in Fig. 4.

The data obtained from VSM measurements are plotted in Fig. 4. In the first five plots (a, b, c, d and e) the complex sample doesn't give distinct paramagnetic signal at room temperature (RT) considering the background diamagnetic signal from the holder and the wax. However, there seems to be some ferromagnetic signal with small coercivity field. At 4 K, there is very distinct paramagnetic signal but after zooming in closely around zero field there seems to be very small coercivity field. These might be because the ferromagnetic signal is still there at 4 K. The magnetization curves of the complex sample at 4 K do not overlap together this is most likely due to the movement of small crystals of the powder in the holder because of the long time vibration resulting from the use of smallest step size when sweeping magnetic field at 4 K. From the last plot (section f), after subtraction of the background signal, complex (2) shows weak paramagnetic behavior at RT and more significant paramagnetic behavior at 4 k. These VSM results reflect that the complex do has unpaired electron spins.

All the VSM data and plots obtained for complexes (2) and (3) are shown in Fig. 5.

In the first two plots (sections a and b), the holder was measured alone and shows a small diamagnetic signal, then the sample straw was measured and shows very small signal similar to large extent to the signal of the system coil (around zero moment) so they will not affect the sample signal. When complex sample measured at room temperature (305 K) it gives "Diamagnetic signal" slightly differs from its holder signal. The diamagnetism of the complex sample means that material induces magnetic field under influence of external field but in opposite direction to it so those are repelled by external magnets and those materials have magnetic permeability less than that of vacuum (μo) (i.e. ≤ 1) and their magnetic susceptibility ≤ 0 so they have ($-$ve) magnetic susceptibility also materials show diamagnetism when there is no unpaired electrons. From these we can conclude that: The metal ion in the ground state may be in the square planar or tetrahedral form and there is no unpaired electrons but if it was in the excited state at room temperature and still diamagnetic this may be due to dimerization this isn't completely clear till now as the chemical structure for the complex not completely defined [17]. The Schiff-base ligands coordinate to Mn(II), Ni(II), Co(II), Cu(II), Pd(II), and Zn(II) ions in a tetra dentate manner using N_2O_2 chromophores. They assigned 4-coordinate square-planar geometry to Cu(II) complexes and tetra-

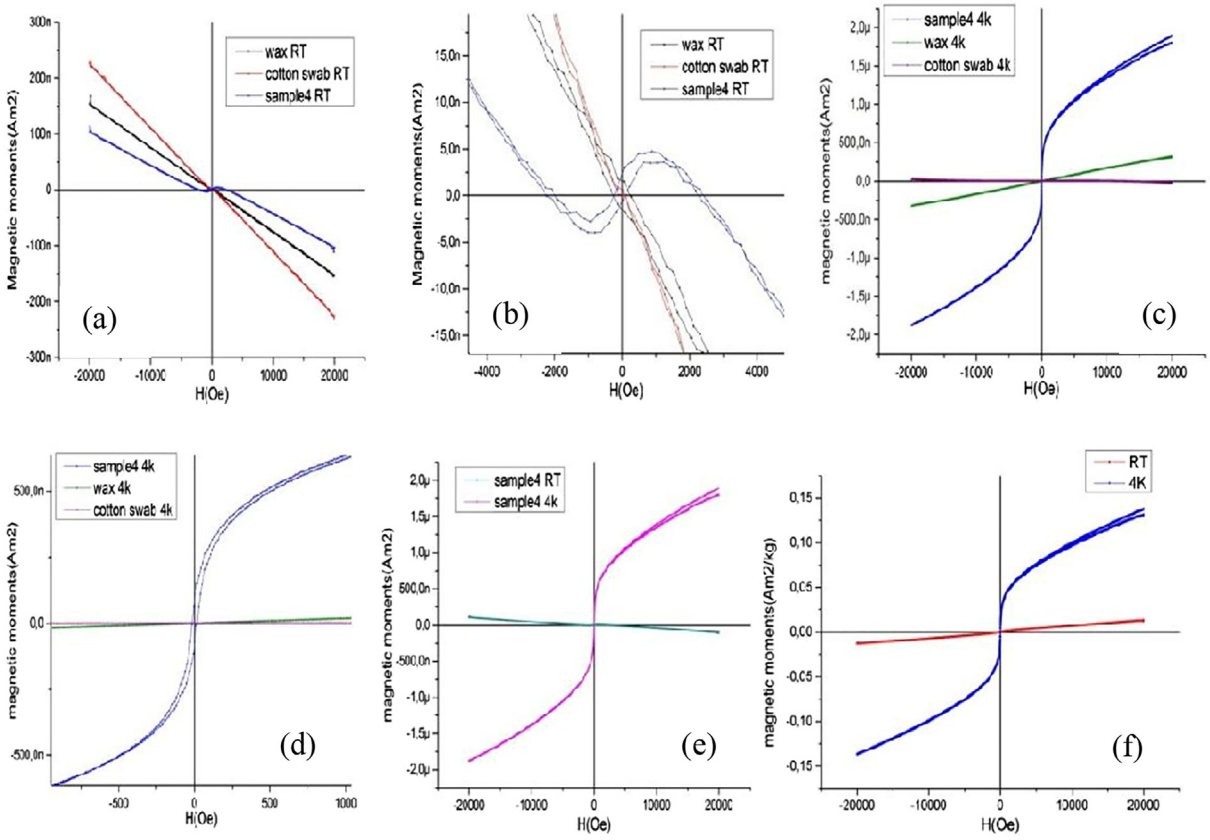

Fig. 4. VSM plots for Complex (2) at RT and 4 K.

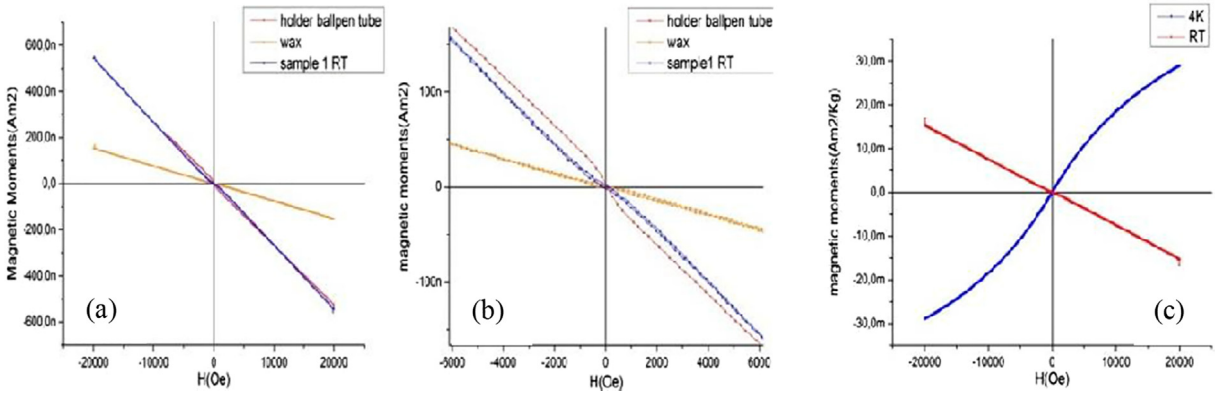

Fig. 5. VSM plots for Complex (3) at RT and 4 K.

hedral geometry to Ni(II) and Co(II) complexes these structures are corroborated by elemental analysis, thermal, magnetic, and electronic spectral measurements [18]. From these investigations the more probable geometry for complex (3) is the tetrahedral. And from the elemental analysis results the more accepted expected structure for complex (3) is $(2L + M.(AC)_2)$.

From third plot (section c), the complex shows diamagnetic behavior at RT and weak paramagnetic behavior at 4 K so the complex may be in the ground state has unpaired electron spin and has the structure of (2L + M.(AC)) and this agrees to great extent to the elemental analysis results.

3.6. Electrical conductivity

Organic Field-Effect-Transistor (OFET) Method: The organometallic complex junctions were made by drop-casting DMSO solutions of the complex onto the interdigitated electrodes (Pt). Together with the measurement results, there are also AFM (atomic force microscopy) pictures of the electrodes before and after the drop-casting. The backside of the devices is p++ silicon which was used as the back-gate. In addition, for some junctions, the light effect on the conductivity was checked. All the measurements were done at RT in vacuum (E-5 ~ E-6 mbar). For the drop-casting of complex (3) solution in DMSO the complex dissolved very well in DMSO (6.0 mg of the complex in 3 mL DMSO) after about 10 days, the solution was still very clear then drop-casting and slow baking carried out at (120 °C) and material dried and filled in the gaps between the interdigitated metal fingers. The AFM pictures of the IDT electrodes for junction 39 gaps, ~70 nm gap spacing and ~8,1 μm long junction are shown in Fig. 6. Sections 6a & 6b before and after drop casting while 6c is the IV characteristic signal for this junction. 2a, 2b and 2c junctions are in the same

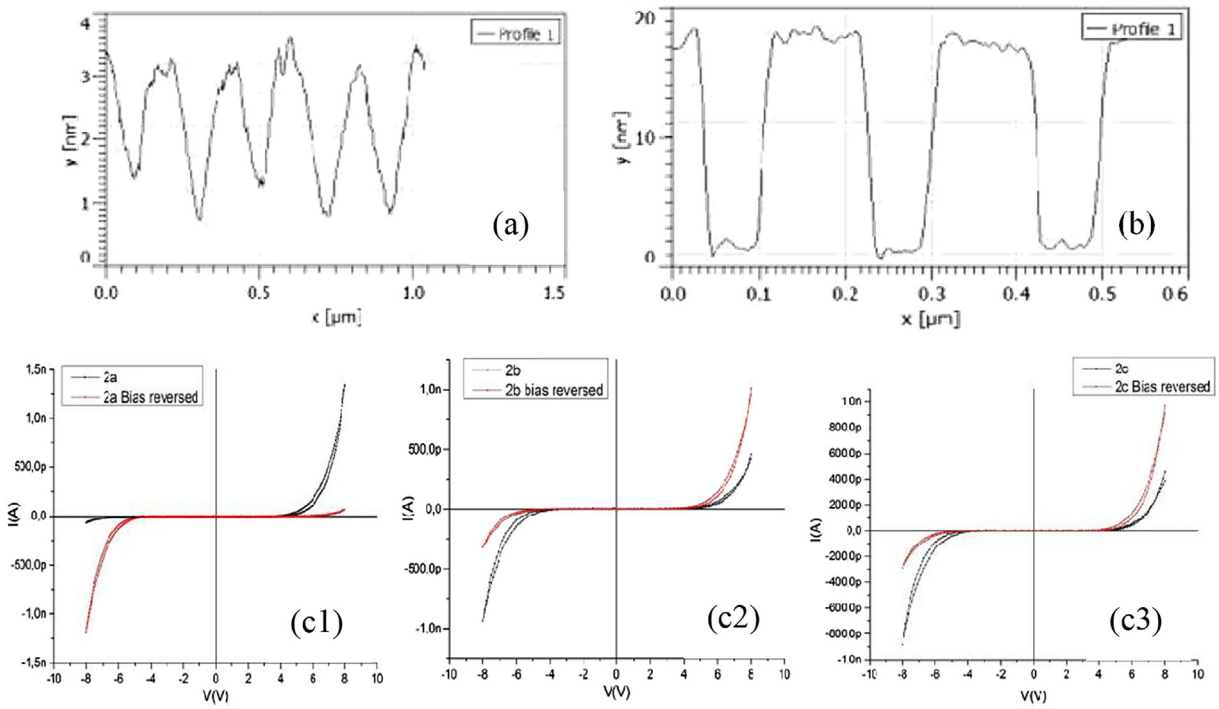

Fig. 6. Complex (3): AFM pictures of IDT electrodes at 39 gaps, ~70 nm gap spacing, ~8.1 µm long (a) before drop casting (b) after drop casting (c1) (IV) characteristic signal junction (2a) at 8 V (300 ms wait) (c2) (IV) characteristic signal junction (2b) at 8 V (1 s wait) (c3) (IV) characteristic signal junction (2c) at 8 V (1 s wait).

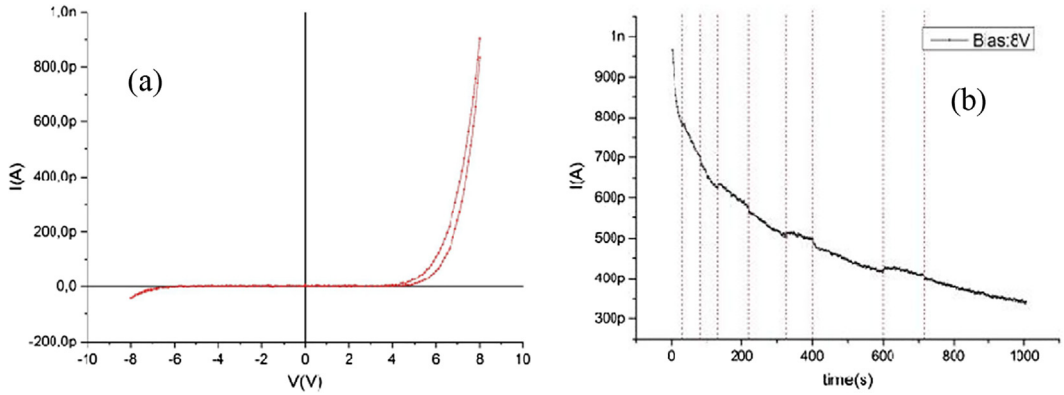

Fig. 7. Complex (3) at 8 V at 39 gaps, ~70 nm gap spacing, ~8.1 µm long (a) (IV) characteristic signal for the light effect junction (2a). (b) Junction (2b).

set. Only 2a junction1 is shown in Fig. 6 section (b) (after drop-casting). The IV characteristic signal for complex (3) (2a, 2b & 2c) junctions were obtained as shown in Fig. 6 (c1) for junction (2a) after 300 ms wait, (c2) for (2b) junction after 1s wait and (c3) for (2c) junction after 1s wait.

The light effect of complex (3) (2a) junction was also studied as shown in Fig. 7.

The effect of changing gap spacing is illustrated in the supporting material.

From all previous figures and data for the electrical transport measurements for complex (3) it is seen that the IV curves are asymmetric. When the bias direction is reversed, the IV curves were also reversed, except at AFM pictures of the IDT electrodes 39 gaps; ~40 nm gap spacing; ~8,1 µm long; When waiting time of each data point is 1s, the hysteresis loop is still distinct. The results of the light effect on the complex junctions 2a &1e and the light effect at bias of 8 V & 5 V respectively, show the time sweeping when applying constant biases. The discharging time is very long, which is in agreement with the hysteresis behavior mentioned above. The light effect was also checked and it was found that there is a little photocurrent when shining light on the device. The gate effect measurement results of the junctions (1a & 3b) demonstrate p-type behavior of the junctions. So the main conclusion is that complex (3) junctions are conducting and show p-type property, but the transport of the junctions has large hysteresis.

4. Conclusions

The conductivity measurement results for complex (1) show that the ionic complex is conducting and non-linear, complex (3) junctions are conducting and show p-type property, but the transport of the junctions has large hysteresis. The VSM measurements of complex (1) show paramagnetic signal at RT (32 °C) or (305 K)

and "S" shaped plot without hysteresis loop at 4 K. Complex (2) shows paramagnetic behavior at RT and the signal increases at 4 K .For complex (3) it shows weak paramagnetic behavior at 4 K and the tetrahedral geometry is the most probable geometry for it.

Declaration of Competing Interest

The authors declare that they have no known competing financial interests or personal relationships that could have appeared to influence the work reported in this paper.

Acknowledgments

The authors would like to thank the Global Young Academy for their financial support for North-South Interdisciplinary Research Grant (One dimensional molecular wires using tailored-to- the purpose chemistry). Also a great thanks to Prof. Wilfred v. d. Wiel, C. H.-H. Traulsen, B. Xu, T.Dogan and C.P. Lawrence team members of the University of Twente for their help in chemical, electrical and magnetic characterizations of the compounds, thanks also to Ayman Mohamed and Ahmed Abdelkawy from Ain Shams University for their help in compounds chemical synthesis.

Appendix A. Supplementary material

Supplementary data to this article can be found online at https://doi.org/10.1016/j.asej.2020.12.002.

References

[1] Layfield RA. Organometallic Single-Molecule Magnets. Organometallics 2014;33:1084.
[2] Miller JS. Magnetically ordered molecule-based materials. Chem Soc Rev 2011;40:3266.
[3] Tamaki H, Zhong Z, Matsumoto J, Kida N, Koikawa S, Achiwa M, et al. Design of metal-complex magnets, syntheses and magnetic properties of mixed-metal assemblies {NBu_4[$MCr(ox)_3$]}x (NBu4+ = tetra(n-butyl)ammonium ion; ox2- = oxalate ion; M = Mn2+, Fe2+, Co2+, Ni2+, Cu2+, Zn2+). J Am Chem Soc 1992;114:6974.
[4] Ni ZH, Zhang LF, Cui AL, Kou HZ. Synthesis, crystal structures and magnetic properties of cyanide-bridged macro cyclic complexes. Sci China, Ser B Chem 2009;52:1444–50.
[5] Beauvais LG, Long JR. $Co_3[Co(CN)_5]_2$: a micro porous magnet with an ordering temperature of 38 K. J Am Chem Soc 2002;124(41):12096–7.
[6] Tuna F, Golhen S, Ouahab L, Sutter J-P. Crystal structure and magnetic properties of $[\{Co(H_2O)_2\}_2Mo(CN)_8]\cdot 4\ H_2O$, a three-dimensional cyanide-bridged bimetallic compound. Elsevier 2003;6(3):377–83.
[7] S. Tabassum, S. Govindaraju, R.-U. Khan, M.A. Pasha, Ultrasound mediated, iodine catalyzed green synthesis of novel 2-amino-3-cyano-4H-pyran derivatives, Ultrasonics Sonochem., Elsevier (24) (2015) 1–7.
[8] Mansoor SS, Logaiya K, Aswin K, Sudhan PN. An appropriate one-pot synthesis of 3,4-dihydropyrano[c] chromenes and 6-amino-5-cyano-4-aryl-2-methyl-4Hpyrans with thiourea dioxide as an efficient, reusable organic catalyst in aqueous medium. J. Taibah Univ. Sci. 2015;9(2):213–26.
[9] Heravi MM, Mousavizadeh F, Ghobadi N, Tajbakhsh M. A green and convenient protocol for the synthesis of novel pyrazolopyranopyrimidines via a one-pot, four-component reaction in water. Tetrahedron Lett, J Polycyclic Aromatic Compd 2014;55(6):1226–8.
[10] Madkour HMF, Afify AAE, Elsayed GA, Salem MS. Use of enaminonitrile moiety in heterocyclic synthesis. Bulgarian Chem Commun 2008;40(2):147–59.
[11] Elziaty AK, Mostafa OEA, El-Bordany EA, Nabil M, Madkour HMF. Access to new pyranopyrazoles and related heterocycles. Int J Sci Eng Res 2014;5(1):727–35.
[12] Elziaty AK, Bassioni G, Hassan AMA, Derbala HA, Abdel-Aziz MS. A synthetic approach to pyrazolopyranopyrimidinones and pyrazolopyranooxazinones as antimicrobial agents. J Chem 2016;5286462. article ID 5286462, p3.
[13] Tanaka K, Shimoura R, Caira MR. Synthesis, crystal structures and photochromic properties of novel chiral Schiff base macrocycles. Elsevier, Tetrahedron Lett 2010;51(2):449–52.
[14] Khalaf MI, Abdo A, Kandil F, Adnan AN. Knoevenagel condensation of some 5-substituted furan-2-carboxaldehyde with creatinineand their antimicrobial Screening. Int J ChemTech Res 2012;4(4):1268–75.
[15] Xavier A, Srividhya N. Synthesis and study of Schiff base ligands. IOSR J Appl Chem (IOSR-JAC) 2278–5736 2014;7 (11): Ver. I, 6–15.
[16] https://en.m.wikipedia.org/wiki/Paramagnetism.
[17] https://chem.libretexts.org/Courses/University_of_California_Davis/UCD_Chem_002C/UCD_Chem_2C%3A_Larsen/Text/Unit_2%3A_Coordination_Chemistry/2.11%3A_Magnetic_Behavior_of_Complex_Ions.
[18] Osowole AA. Synthesis, characterization, and magnetic and thermal studies on some metal (II) thiophenyl schiff base complexes. Int J Inorg Chem 2011;2011: Article ID 650186.

Rehab Ibrahim Yousef (1991), graduated from Faculty of Science, Chemistry Department, Ain Shams University 2012 (very good with honor grade). Worked for one year (2013-2014) as teaching assistant in the chemistry department at Faculty of Engineering, Ain Shams University. Finished premaster studies in physical chemistry and registered for Master studies since 2015. Organizer for the Workshop on Oil field Chemistry (WOC) which was held in the Faculty of Engineering at Ain Shams University in 2014 and 2017.

Naglaa Fawzy H. Mahmoud, MSc., PhD, Associate Professor of Organic Chemistry 27 Years' Experience in teaching Organic Chemistry to both under and post graduates. Also, develop, lead and supervise research work qualifies for MSc. And PhD degrees. Active member in Egyption chemical society for heterocyclic compounds and International Society of applied chemistry. Extensive experience in putting and executing research plans for post graduates in Organic Chemistry field. Very experienced in operating Advanced Lab Apparatuses and interpret its output reports, e. ^{1}H-NMR, IR, ^{13}C-NMR. . .etc. Fully aware of Research Methods, Scientific Technical Writing protocols, and Library Search Processes in support of extracting research points.

Fouad Ibrahim El-hosiny (1952) graduated from the Faculty of Science 1980 and occupy demonstrator position at chemistry department at Faculty of Science, Ain shams University. Obtained his M.Sc degree in chemistry from the Faculty of Science, Ain Shams University in 1984 and occupied teaching assistant position at the faculty in 1985. Obtained his Ph.D in chemistry from the Faculty of Science, Ain Shams University in 1988.Associate professor in 1995. Professor at the physical chemistry department at the Faculty of Science In 2003 Ain Shams University. And occupied the Head of the physical chemistry department till now.

Fritz E. Kühn received his doctoral degree at the Technische Universität München (TUM, Germany) in 1994, and worked at Texas A&M University (USA) as postdoctoral research associate. After that he executed his "Habilitation" at TUM between 1996 and 2000. In 2002 he started lecturing at TUM Asia, a joint venture of the National University of Singapore (NUS) and TUM. In 2005 he accepted a position as principal investigator at the Instituto Technologico e Nuclear (ITN) in Sacavem (Portugal). In 2006 he was appointed Professor of Molecular Catalysis at TUM and returned to Germany. Fritz Kühn has also given lectures at the Nanjing Technological University in China for a couple of years and was appointed Visiting Professor at NUS (Singapore) in 2008. Fritz Kühn is departmental Dean of Internationalization since 2007, Faculty Graduate Dean since 2010, Member of the Board of TUM Create (Singapore) since 2012 and Dean of Studies since 2016. Focus of his research is on organometallic chemistry and its application in molecular catalysis, bio-inspired chemistry and medicinal chemistry. Fritz Kühn has received several awards for his scientific work, is author or co-author of more than 490 scientific publications and ca, 20 patens. His h-index is currently 61.

Ghada Bassioni, Ph.D. (Dr. rer. nat.), 2004, Technical University Munich, Germany. She is a Professor and the Head of the Chemistry Division at the Faculty of Engineering, Ain Shams University in Cairo and is a member of the Egyptian National Committee of Pure and Applied Chemistry and has been recently elected to the Bureau of the International Union of Pure and Applied Chemistry (IUPAC). She is an international project officer at the Science and Technology Development Fund (STDF), Egyptian Ministry of Scientific Research and has been a member of the Global Young Academy from 2013-2018. She has over 70 scientific publications in peer-reviewed journals and conference proceedings and has been recognized with several national (like the Egyptian State Incentive Award in Chemistry, 2013), regional (like the LEWA Leadership Excellence for Women runner up award, 2013) and international awards (like the Young Scientist Award at the World Economic Forum in Dalian, 2013) and was selected as an academic visitor and panelist at the Nobel Laureates meetings in Lindau, Germany, in 2012 and 2014, respectively. In 2016, she has been awarded the Next Einstein and the Fulbright fellowships as well as the L.A.B. fellowship of three organizations: Nobel Laureate Meetings in Lindau, the European Forum in Alpbach and the Falling Walls in Berlin.